

RESEARCH

Open Access



Combinative effects of akarkara root-derived metabolites on anti-inflammatory and anti-alzheimer key enzymes: integrating bioassay-guided fractionation, GC-MS analysis, and *in silico* studies

Rana M. Ibrahim^{1†}, Passent M. Abdel-Baki^{1*†}, Ghada F. Elmasry^{2*}, Ahmed A. El-Rashedy³ and Nariman E. Mahdy¹

Abstract

Background *Anacyclus pyrethrum* L. (Akarkara root), a valuable Ayurvedic remedy, is reported to exhibit various pharmacological activities. Akarkara root was subjected to bioassay-guided fractionation, to isolate its active constituents and discover their potential bioactivities, followed by computational analysis.

Methods The methanol extract and its fractions, methylene chloride, and butanol, were assessed for their antioxidant, anti-inflammatory, and anticholinergic potentials. The antioxidant activity was determined using DPPH, ABTS, FRAP, and ORAC assays. The *in vitro* anticholinergic effect was evaluated via acetyl- and butyryl-cholinesterase inhibition, while anti-inflammatory effect was determined using COX-2 and 5-LOX inhibitory assays. The methylene chloride fraction was subjected to GC/MS analysis and chromatographic fractionation to isolate its major compounds. The inhibitory effect on iNOS and various inflammatory mediators in LPS-activated RAW 264.7 macrophages was investigated. *In silico* computational analyses (molecular docking, ADME, BBB permeability prediction, and molecular dynamics) were performed.

Results Forty-one compounds were identified and quantified and the major compounds, namely, oleamide (**A1**), stigmaterol (**A2**), 2E,4E-deca-2,4-dienoic acid 2-phenylethyl amide (**A3**), and pellitorine (**A4**) were isolated from the methylene chloride fraction, the most active in all assays. All compounds showed significant *in vitro* antioxidant, anticholinergic and anti-inflammatory effects. They inhibited the secretion of pro-inflammatory cytokines (TNF- α , IL-1 β , and IL-6) in activated RAW macrophages. The isolated compounds showed good fitting in the active sites of acetylcholinesterase and COX-2 with high docking scores. The ADME study revealed proper pharmacokinetics and

[†]Rana M. Ibrahim and Passent M. Abdel-Baki contributed equally to this work.

*Correspondence:
Passent M. Abdel-Baki
passent.mohamed@pharma.cu.edu.eg
Ghada F. Elmasry
ghada.elmasry@pharma.cu.edu.eg

Full list of author information is available at the end of the article



© The Author(s) 2023. **Open Access** This article is licensed under a Creative Commons Attribution 4.0 International License, which permits use, sharing, adaptation, distribution and reproduction in any medium or format, as long as you give appropriate credit to the original author(s) and the source, provide a link to the Creative Commons licence, and indicate if changes were made. The images or other third party material in this article are included in the article's Creative Commons licence, unless indicated otherwise in a credit line to the material. If material is not included in the article's Creative Commons licence and your intended use is not permitted by statutory regulation or exceeds the permitted use, you will need to obtain permission directly from the copyright holder. To view a copy of this licence, visit <http://creativecommons.org/licenses/by/4.0/>. The Creative Commons Public Domain Dedication waiver (<http://creativecommons.org/publicdomain/zero/1.0/>) applies to the data made available in this article, unless otherwise stated in a credit line to the data.

drug likeness properties for the isolated compounds. The isolated compounds demonstrated high ability to cross the BBB and penetrate the CNS with values ranging from 1.596 to -1.651 in comparison with Donepezil (-1.464). Molecular dynamics simulation revealed stable conformations and binding patterns of the isolated compounds with the active sites of COX-2 and acetyl cholinesterase.

Conclusions Ultimately, our results specify Akarkara compounds as promising candidates for the treatment of inflammatory and neurodegenerative diseases.

Keywords Akarkara root, GC-MS, Anti-inflammatory, Anticholinergic, Molecular docking, ADME

Background

Non-communicable diseases are becoming more common throughout the world and tend to be of long duration. They are the result of a combination of genetic, physiological, environmental, and behavioral factors like Alzheimer's disease (AD), cancers, diabetes, and chronic cardiovascular diseases. AD is a progressive, age-related neurodegenerative condition that affects the elderly. Memory loss, a deterioration in language abilities, and other cognitive deficits are characteristics of AD. Around 50 million people are estimated to have dementia according to the World Health Organization (WHO), with AD being the most prevalent form, accounting for 60–70% of all cases. It is concerning because 82 million people are anticipated to experience AD globally by 2030 and 152 million by 2050 [1]. One of the major difficulties facing healthcare systems is the financial impact of dementia in terms of direct medical and social care expenditures. According to The World Alzheimer Report (2015), the expense of caring for AD patients would reach 2 trillion US\$ by 2030, undermining global social, and economic advancement besides, overwhelming health and social services, including long-term care systems [2]. Oxidative stress is the main obstacle in the majority of diseases. The imbalance between the generation of free radicals and reactive metabolites starts to destroy vital cells and biomolecules, potentially having an impact on the health of the entire body. An antioxidant defense mechanism is any defensive mechanism that eliminates such free radicals [3]. By synchronizing the destructive activity of free radicals, the antioxidant defense mechanism plays a crucial part in reducing free radicals. They mainly target macromolecules that damage cells [4]. The etiology of AD is significantly influenced by these oxidative stress, inflammation and decreased acetylcholine levels [5, 6]. As a result, treating high levels of oxidative stress prevents the progression of numerous disorders, including Alzheimer's disease [7]. There are many theories have been proposed for the pathophysiology of AD, such as dysfunction of the cholinergic neurons system, deposits of β -amyloid ($A\beta$) protein, τ -protein hyperphosphorylation, and metal dyshomeostasis [8]. According to the cholinergic hypothesis, increasing acetylcholine levels in the brain by blocking cholinesterase enzymes is an

effective therapeutic strategy for treating the symptoms of Alzheimer's disease. This is achieved through inhibiting acetyl- (AChE) and butyryl-cholinesterase (BChE). However, this therapeutic strategy simply provides symptomatic alleviation rather than a drastic cure, failing to stop or considerably slow the disease's course [9]. Neuroinflammation triggered by inflammatory mediators such as prostaglandins [by cyclooxygenase-2 (COX-2)], leukotrienes [by 5-lipoxygenase (5-LOX)], and nitric oxide [by inducible nitric oxide synthase (iNOS)], as well as pro-inflammatory cytokines [tumor necrosis factor-alpha (TNF- α), and interleukins (IL-1 β and IL-6)] has been shown to play a role in the etiology of AD [10], along with oxidative stress [8]. Free radicals are produced in greater quantities when an inflammatory process begins in the body. Consequently, it is preferable to provide the patient with a suitable antioxidant as an additional treatment for Alzheimer's and neuroinflammation. Drugs that modify the activity of a particular target may not be sufficient to stop the course of AD due to the complexity of the illness. Therefore, the development of multi-targeted medications that combine various pharmacological actions is more likely to result in effective therapy.

Anacyclus pyrethrum L. (Asteraceae), commonly known as Akarkara, is native to Asia and Africa [11]. The roots and leaves of the plant are well documented in Ayurvedic and Unani systems of holistic healing. *A. pyrethrum* is used as a brain tonic in complementary and alternative medicine [12]. In traditional North African and Indian medicine, *A. pyrethrum* roots are used to treat several diseases, including Alzheimer's disease, diabetes, anabolic, aphrodisiac, reproductive, anti-rheumatic, analgesic, antibacterial, antiviral, carminative, anti-catarrhal, digestion, febrifuge, nervine, vermifuge, and sialagogue [13, 14]. In Indian ayurvedic medicine, it is widely used for the treatment of male infertility [15]. In siddha medicine, it is used for treatment of arthritis [16]. It is widely used in the treatment of epilepsy, seizures and lung infections, as well as its use as an insecticide in ethnomedicines [17]. *A. pyrethrum* roots were reported to exhibit memory-enhancing, anticonvulsant, antioxidant, neuropharmacological, anti-inflammatory, analgesic, wound healing, immunostimulant, antibacterial, androgenic, antiplasmodial and insecticidal activities [13, 18,

19]. Several interesting active constituents were reported in *A. pyrethrum* including pyrethrins, alkylamides, and polysaccharides [19]. Despite the various ethnopharmacological and phytotherapeutic reports regarding its neuropharmacological, anti-inflammatory, and antioxidant activities, nothing was traced about its potential as a multi-targeted AD drug.

There is a significant shift in drug discovery from synthetic moieties to herbal formulations for the treatment of neurological disorders and their scientific validation to cure neurodegenerative disorders. Therefore, this study was conducted to highlight the beneficial effects of *A. pyrethrum* roots as antioxidant, anti-inflammatory, and anticholinergic drug that can be used to prevent or manage the symptoms or halt the progression of neurodegenerative diseases. The methanol extract (ME) of the roots and its fractions [methylene chloride (MCF) and butanol (BF)] were tested for their antioxidant capacities using different methods, such as DPPH (2,2-diphenyl-1-picrylhydrazyl), ABTS (2,2'-azino-di(3-ethylbenzthiazoline-6-sulfonic acid), FRAP (ferric reducing antioxidant power), ORAC (oxygen radical absorbance capacity), and metal chelation assay. Furthermore, the *in vitro* anticholinergic (AChE and BChE) and anti-inflammatory (COX-2 and LOX) effects of all extracts were evaluated. Furthermore, the effects of Akarkara root extract, its fractions, and isolated compounds on cell viability of RAW264.7 macrophages were assessed by MTT (3-[4,5-dimethylthiazol-2-yl]-2,5 diphenyl tetrazolium bromide) assay. The inhibition of iNOS and pro-inflammatory cytokines (TNF- α , IL-1 β , and IL-6) were evaluated in lipopolysaccharides (LPS)-induced RAW264.7 macrophages model. After that, GC-MS analysis of the most active fraction was conducted for qualitative and quantitative estimation of its chemical composition, followed by a bioassay-guided fractionation to isolate its major active constituents, and explore their potential biological activities. Additionally, the potential binding modes and interactions of the isolated compounds with AChE and COX-2 active sites were studied using molecular docking to investigate better the mode of interaction underlying the inhibitory effects for the first time. Further, ADME computational parameters were studied *in silico* to predict the physicochemical properties of the isolated compounds. Finally, a molecular dynamic simulation was carried out to predict the performance of the isolated compounds upon binding to the active sites of AChE and COX-2, as well as their interaction and stability through the simulation. These findings may claim the multi-targeted potential of *A. pyrethrum* and its isolates against AD for the first time.

Materials and methods

Plant material

Akarkara (*Anacyclus pyrethrum* L.) roots were obtained from a local market (Harraz for Food Industry and Natural Products, Egypt) in March 2021 and authenticated by Mrs. Teresa Labib, Head of the Taxonomists at Orman Botanic Garden. This study complies with local, national, and international guidelines, and no specific consent was required for the collection of the plant material.

Preparation and fractionation of the methanolic extract (ME)

The preparation and fractionation of the methanolic extract (ME) were done according to a previously published method with slight modifications [20]. Akarkara roots (5 kg) were dried, powdered, and extracted with methanol in soxhlet apparatus. The ME was evaporated under reduced pressure by vacuum distillation at a temperature not exceeding 50 °C. The residue (350 g) was suspended in water and subjected to liquid-liquid fractionation with methylene chloride (5×500 mL) followed by *n*-butanol saturated with water (5×500 mL). The collected solvent was evaporated under reduced pressure at a temperature not exceeding 50 °C to yield methylene chloride (MCF) (50 g) and butanol (BF) (44 g) fractions, respectively. The MCF was subjected to further bioassay-guided isolation procedures.

Isolation of the major compounds from the methylene chloride fraction (MCF)

The MCF (30 g) was chromatographed on silica gel H 60 (500 g) using a vacuum liquid chromatography column (VLC) (25 L × 7 D cm). The detailed chromatographic fractionation and isolation scheme is illustrated in Fig. S2. The details of the purification and isolation of each compound are recorded in the supplementary.

Methods

The detailed procedures are described in the [Supplementary online resource](#).

Results and discussion

Antioxidant and metal chelating activity of ME, MCF, and BF

The generation of free radical species by oxidative stress as well as metal dyshomeostasis are crucial factors in the development of AD. Thus, antioxidants may help to prevent these processes, supporting anti-AD medication. The antioxidant, as well as metal chelating activity of the ME, MCF, and BF were assessed using five different *in vitro* assays viz.; radical scavenging activity [DPPH, ABTS, redox potential (FRAP), ORAC, and metal chelating assay (Fig. 1A-C). The IC₅₀ values of the tested samples were determined using the DPPH assay using

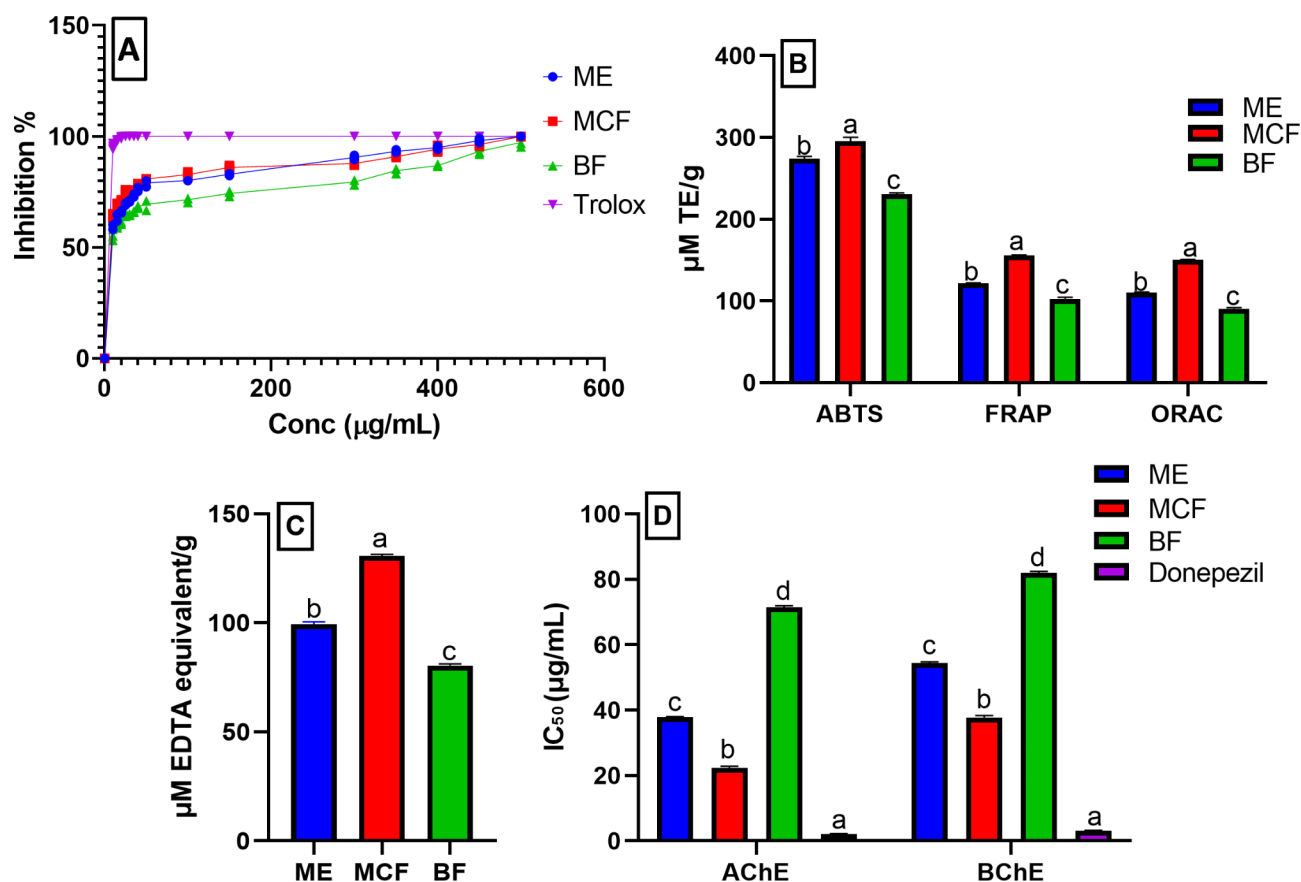


Fig. 1 Antioxidant activity of *A. pyrethrum* roots methanolic extract (ME), methylene chloride (MCF), and butanol (BF) fractions using (A) DPPH represented by a line graph, (B) ABTS, FRAP, and ORAC, (C) metal chelating assay, and (D) anticholinergic activity (AChE and BChE). μM : micromolar; TE: Trolox; Data are expressed as mean \pm standard deviation of three replicates; equivalent. Different letters on the bar indicate significant differences at $P < 0.0001$ with Tukey's test

Trolox as a standard (IC_{50} 1.41 ± 0.08 $\mu\text{g/mL}$). Herein, the MCF showed the highest antioxidant potential with IC_{50} 10.60 ± 0.1 $\mu\text{g/mL}$, followed by the ME and BF (IC_{50} 13.78 ± 0.2 and 17.73 ± 0.16 $\mu\text{g/mL}$, respectively). The results were in accordance with previous literature determining the IC_{50} of *A. pyrethrum* methanolic extract (12.38 ± 0.25 $\mu\text{g/mL}$) [21] and was higher than that reported for 50% methanolic extract (IC_{50} 467.1 $\mu\text{g/mL}$) [22]. In addition, the MCF exhibited the highest antioxidant potential equivalent to 295 ± 5.14 $\mu\text{M TE/g}$ (ABTS), 155.3 ± 0.70 $\mu\text{M TE/g}$ (FRAP), 150.6 ± 0.32 $\mu\text{M TE/g}$ (ORAC). Also, it showed the highest metal chelating activity explaining 130.7 ± 0.72 $\mu\text{M EDTA equivalent/g}$. These results suggested that MCF might have potential preventive values against AD and other oxidative-induced diseases. The in vivo antioxidant potential of the plant is well documented in literature [23]. Its antioxidant potential has been correlated with its traditional uses as anticonvulsant, brain tonic [24], anti-inflammatory [25], preventing oxidative DNA damage and cytotoxicity [22], anti-diabetic [26]. Further investigation could potentially

lead to the discovery of phytochemicals with promising antioxidant and anti-neurodegenerative activities.

Anticholinergic activity of ME, MCF, and BF

The main cholinesterase enzymes that significantly contribute to the hydrolysis and control of acetylcholine are AChE and BChE. Thus, inhibition of these enzymes increases the level of acetylcholine in the brain. In addition, numerous studies have highlighted the chaperone function of AChE through its peripheral anionic site in boosting the neurotoxicity of amyloid- β (Ab) fibrils and promoting their production [9]. Therefore, ChE inhibitors that simultaneously block the peripheral anionic and catalytic sites of AChE as well as the catalytic activity of BChE may have a double benefit, enhancing cholinergic transmission and possibly delaying the production of the extracellular plaques [27]. There are numerous ongoing researches for the discovery of natural anticholinergic drugs from plant sources. As most of the drugs currently available for the treatment of Alzheimer's disease, such as rivastigmine and galanthamine are derived from natural products. It is worth mentioning that the

AChE inhibitory activity of *A. pyrethrum* roots ethanolic extract was previously reported, recommending its use as anticholinergic [27]. Thus, the AChE and BChE inhibitory activities of the ME, MCF, and BF were determined (Fig. 1D). Herein, the MCF exhibited the highest inhibition of both AChE and BChE with the lowest IC_{50} (concentration required to inhibit 50% of the enzyme activity) corresponding to 22.4 ± 0.45 and 37.75 ± 0.65 $\mu\text{g/mL}$, compared to donepezil (IC_{50} 2.15 ± 0.13 and 3.15 ± 0.18 , respectively). This potent inhibition suggested that MCF may be a candidate for the treatment of Alzheimer's disease. Further chemical investigation of its component metabolites might guide the discovery of various cholinesterase inhibitors.

In vitro anti-inflammatory activity of ME, MCF, and BF

Neuroinflammation is a major pathological aspect of AD as it leads to neurodegeneration. This is brought on by the increase of the inflammatory proteins (COX-2 and LOX), being expressed in the neuronal regions of the brains in AD patients [28]. Cyclooxygenase (COX-2) is a bi-functional enzyme that first catalyzes the addition of two molecules of oxygen to arachidonic acid to form the hydroperoxide, prostaglandin G_2 (PGG_2), and then reduces the latter to alcohol (PGH_2), by peroxidase activity. Prostaglandins (PGs) are considered important biological mediators of inflammation, originating from the biotransformation of arachidonic acid catalyzed by cyclooxygenase. Thus, the inhibition of COX-2 enzyme will mediate anti-inflammatory actions by interfering with prostaglandin production [29, 30]. The concentration of tested samples causing 50% COX-2 inhibition (IC_{50}) was calculated and compared to the standard Celecoxib (Fig. 2A). Moreover, the ability of the tested samples to inhibit 5-Lipoxygenase enzyme was investigated, which may have significant pro- or anti-inflammatory activity in AD. As, the lipoxygenases (LOXs) involve in the

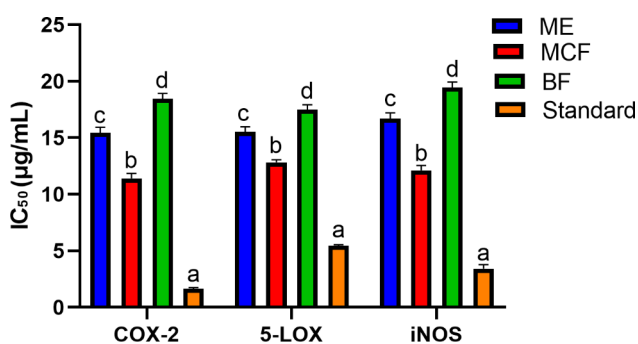


Fig. 2 Anti-inflammatory activities of *A. pyrethrum* roots methanolic extract (ME), methylene chloride (MCF), and butanol (BF) fractions in vitro against COX-2 and 5-LOX, as well as in LPS-induced RAW264.7 macrophages (iNOS). Different letters on the bar indicate significant differences at $P < 0.0001$ with Tukey's test. Standards: Celecoxib (COX 2), Zileuton (5-LOX), and parthenolide (iNOS) are serving as positive controls

biosynthesis of leukotrienes and catalyze the addition of oxygen to linolenic, arachidonic (AA), docosahexaenoic acids (DHA), and other polyunsaturated fatty acids leading to the formation of bioactive lipids, significantly affect the course of neurodegenerative diseases [10]. However, inhibition of COX-2 shifts arachidonic acid metabolism from prostaglandins synthesis to leukotriene synthesis via upregulation of 5-LOX, resulting in increased levels of leukotrienes [31]. Therefore, dual COX-2/5-LOX inhibitors constitute an emerging therapy for inflammation. Thus, 5-LOX inhibitory activity of the tested samples was assessed in comparison to the standard Zileuton (Fig. 2A) and their IC_{50} values were determined.

The MCF showed the highest inhibition among tested samples against COX-2 (IC_{50} 11.4 ± 0.46 $\mu\text{g/mL}$) compared to Celecoxib (IC_{50} 1.65 ± 0.10 $\mu\text{g/mL}$). It also exhibited the highest 5-LOX inhibitory potential (IC_{50} 12.82 ± 0.23 $\mu\text{g/mL}$) compared to the standard Zileuton (IC_{50} 5.44 ± 0.11 $\mu\text{g/mL}$). The results of the anti-inflammatory activity of MCF were correlated with its respective antioxidant and anticholinergic activities, which may aid in the development of novel therapies to relieve or prevent neurodegenerative disorders associated with AD.

Cell viability on RAW264.7 macrophages

In MTT assay, the extract and fractions did not show cytotoxic activity (up to 250 $\mu\text{g/mL}$) (Figs. S4A and S5A-C), while the isolated compounds were safe up to 250 μM (Figs. S4B and S5D-G) when assayed on RAW264.7 macrophages (after 24 h incubation), indicating their safety and their potential as candidates for chronic treatment. The results suggest the ideal safety profile of *A. pyrethrum* extract and fractions, which match previous reports shedding light on their safety even for chronic treatments [32].

LPS-induced RAW264.7 macrophages (iNOS) anti-inflammatory activity of ME, MCF, and BF

Macrophages are activated by different factors as pro-inflammatory cytokines and bacterial lipopolysaccharide (LPS). Activated macrophages produce many cytokines such as $\text{TNF-}\alpha$, IL-6, and IL- 1β , among other inflammatory mediators such as NO and PGE_2 [10]. The free radical NO is produced by nitric oxide synthase (NOS), which exists as three isoforms: endothelial NOS (eNOS), inducible NOS (iNOS), and neuronal NOS (nNOS). LPS-stimulated macrophages produce NO by up-regulating iNOS expression through the production of inflammatory cytokines [10]. Thus, inhibition of these inflammatory mediators can be considered an effective strategy for the development of anti-inflammatory drugs. Regarding the inhibition of iNOS in the LPS-induced RAW264.7 macrophages (Fig. 2), MCF showed the highest inhibitory potential with IC_{50} equivalent to 12.11 ± 0.44 $\mu\text{g/}$

mL compared to the standard drug; Parthenolide (IC_{50} 3.44 ± 0.35).

Phytochemical characterization of the biologically active fraction (MCF)

Identification and quantification by GC-MS

As a result of the significant antioxidant, anticholinergic and anti-inflammatory activities of the MCF, compositional analysis of the MCF, was required to identify and quantify its compounds that could be correlated with its highest activities among the studied fractions. As the biological and pharmacological effects of non-polar fractions are frequently attributed to a variety of triterpenoid and steroid compounds [33]. However, these compounds are typically detected as complicated isomeric mixtures. It was proved that GC-MS is the method of choice for identifying triterpenes, sterols, glycerols, waxes, fatty acids, and other chemicals from non- and semi-polar fractions [34]. Several alkylamides have been reported in *Anacyclus* species. The structural resemblance of these amides makes it difficult to separate them from the mixtures. However, GC-MS is a powerful method for extracting known amides from mixtures [35]. Thus, GC-MS post silylation (Fig. S1) was employed for compositional analysis of the MCF. Forty-one compounds were identified and quantified (Table 1) representing 93.36% of the total compounds present. The detected compounds belong to different chemical classes, including terpenes, alkylamides, alkanes, fatty acids, esters, and sterols. Alkylamide was the major class detected, representing 59.59%, where oleamide constituted 17.53%, followed by 2E,4E-deca-2,4-dienoic acid 2-phenylethyl amide (11.22%), and deca-2E,4E-dienoic acid isobutylamide (pellitorine) (7.96%). Sterols represented the second major class, accounting for 12.33% with stigmaterol (8.78%) the predominant sterol. Previously, GC-MS characterization of the ethanolic extract of *A. pyrethrum* roots detected nearly similar classes of compounds including fatty acids, alkylamides, triterpenes, and sterols [36, 37]. Moreover, characterization of the hydroalcoholic extract of *A. pyrethrum* roots, seeds, leaves, and capitula showed the presence of various compounds as sarcosine, N-(trifluoroacetyl)-butyl ester, levulinic acid, malonic acid, palmitic acid, morphinan-6-one,4,5 α -epoxy-3-hydroxy-17-methyl, 2,4-undecadiene-8,10-diyne-N-tyramide, and isovaleric acid [38, 39]. The petroleum ether extract of *A. pyrethrum* roots was rich in fatty acids, esters and sterols [40]. To our knowledge, this is the first profiling and quantitative exploration of the methylene chloride fraction of *A. pyrethrum* roots rather than the total extract by GC-MS. The presence of diverse components in MCF of *A. pyrethrum* roots may be of great significance in various medicinal applications like in AD. Taking into consideration that, it is necessary to identify these compounds. Through

previous studies, alkylamides were proved to exhibit antioxidant and anti-inflammatory activities, as well as being promising candidates for the treatment of neurological diseases such as Alzheimer's. [41]. Previous reports revealed that terpenes (diterpenes, triterpenes and sesquiterpenes) are powerful cholinesterase inhibitors [42]. Triterpenes and sterols have been reported for their anti-inflammatory, anti-cholinesterase, and antioxidant activities, as well as their effectiveness against neurodegenerative disorders [43–45]. Furthermore, organic acids were proved to lower the incidence of neurodegenerative diseases and avoid the risk factors [46]. In addition, fatty acids showed effective management of AD through inhibition of neuroinflammation [47, 48]. As a result, these compounds may contribute to the previously determined antioxidant, anti-inflammatory, and anticholinergic activities of the most promising fraction (MCF).

Isolation of the major compounds

Extensive chromatographic fractionation and purification of the MCF (Fig. S2) was performed with the aim of isolating its major active compounds and evaluating their respective biological potentials, which is then demonstrated by detailed ADME studies. Four compounds (A1–A4) were isolated and identified by their physicochemical characters, NMR-spectroscopic analyses (^1H and ^{13}C), and comparison with the available literature (NMR details are in Supplementary material). The identities of the isolated compounds were confirmed as A1: 9-cis-octadecenamide (oleamide) [49], A2: stigmaterol [50], A3: 2E, 4E-deca-2,4-dienoic acid 2-phenylethyl amide [51] and A4: deca-2E,4E-dienoic acid isobutylamide (pellitorine) [52]. As far as the available literature is concerned, this is the first report on the isolation of oleamide from genus *Anacyclus*. The chemical structures of compounds A1–A4 are illustrated in Fig. S3.

Antioxidant and metal chelating activity of the isolated compounds (A1–A4)

The DPPH radical scavenging assay determined the IC_{50} of the isolated compounds (Fig. 3A). Stigmaterol (A2) showed the highest activity with IC_{50} 16.37 ± 0.23 μM relative to Trolox (IC_{50} 5.63 μM), followed by 2E,4E-dienoic acid 2-phenylethylamide (A3) (IC_{50} 17.73 ± 0.16 μM), oleamide (A1) (IC_{50} 21.67 ± 0.21 μM), and pellitorine (A4) (IC_{50} 22.55 ± 0.41 μM). In addition, three extra assays; ABTS, FRAP, and ORAC were used to assess the isolated compounds' antioxidant activity [53]. The four compounds exhibited high antioxidant potential ranging from 203.46 ± 0.31 to 85.51 ± 0.24 $\mu\text{M TE/g}$ (Fig. 3B). Stigmaterol (A2) showed the highest antioxidant potential followed by deca-2E,4E-dienoic acid 2-phenylethylamide (A3), and oleamide (A1), then pellitorine (A4). The four isolated compounds showed high metal chelating activity

Table 1 The relative percentage of silylated compounds in *A. pyrethrum* root methylene chloride fraction using GC-MS

RT (min)	RI	Compound	Molecular formula	Molecular weight	Relative %	SE	Chemical Class
13.41	1377	Copaene	C ₁₅ H ₂₄	204	1.58	0.09	SC
13.75	1573	Spathulenol	C ₁₅ H ₂₄ O	220	0.40	0.12	SA
15.01	1613	Caryophyllene oxide	C ₁₅ H ₂₄ O	220	0.35	0.28	SO
15.21	1788	N-isobutyl-dodeca-2,4,8,10-tetraenamide	C ₁₆ H ₂₅ NO	247	0.76	0.99	AA
15.40	1802	Hexadecane	C ₁₆ H ₃₄	226	0.49	0.89	A
15.91	1856	Heptadecane	C ₁₇ H ₃₆	240	1.03	0.73	A
16.38	1878	N-isobutyl-2,4-heptadiene-6-monoynamide	C ₁₁ H ₁₅ NO	177	0.48	0.01	AA
16.76	1891	Lauric acid	C ₁₂ H ₂₄ O ₂	200	4.55	0.12	FA
16.96	1900	Myristic acid	C ₁₄ H ₂₈ O ₂	228	0.33	0.55	FA
17.09	1910	Pentadecanoic acid	C ₁₅ H ₃₀ O ₂	242	0.51	0.39	FA
17.61	1921	Palmitic acid	C ₁₆ H ₃₂ O ₂	256	1.56	1.01	FA
18.17	1936	Linoleic acid	C ₁₈ H ₃₂ O ₂	280	0.38	0.04	FA
18.45	1941	Stearic acid	C ₁₈ H ₃₆ O ₂	284	0.18	0.08	FA
19.02		Tetradeca-2E,4E-dien-8,10-diynoic acid isobutylamide (anacycline)	C ₁₈ H ₂₅ NO	271	0.30	0.12	AA
19.87	1946	Deca-2E,4E-dienoic acid isobutylamide (pellitorine)	C ₁₄ H ₂₅ NO	223	7.96	0.22	AA
20.20	1949	Deca-2E,4E,8Ztrienoic acid isobutylamide (8,9-(dehydropellitorine)	C ₁₄ H ₂₃ NO	221	2.33	0.67	AA
20.34	1951	Undeca-2E,4E-diene-8,10-diynoic acid isobutylamide	C ₁₅ H ₁₉ NO	229	0.49	0.78	AA
20.50	1959	Deca-2E,4E,8Ztrienoic acid piperidide	C ₁₅ H ₂₃ NO	233	0.86	0.89	AA
21.04	1976	Tetradeca-2E-diny-8,10-diynoic acid isobutylamide	C ₁₈ H ₂₇ NO	273	0.64	0.99	AA
21.84	1989	Tetradeca-2E,4E, nE-trienoic-8,10-diynoic acid Isobutylamide	C ₁₈ H ₂₃ NO	269	0.24	1.03	AA
23.02	2007	N-isobutyl-2,4-undecadiene-8,10-dynamide	C ₁₆ H ₂₁ NO	243	0.78	0.03	AA
23.11	2018	Dodeca-2E,4E, nE-trienoic acid 4-hydroxyphenylethylamide	C ₂₀ H ₂₇ NO ₂	313	0.46	0.06	AA
23.43	2029	2,8-N-isobutyl-2,8-dodecadienamide	C ₁₆ H ₂₉ NO	251	0.92	0.82	AA
23.59	2041	Tetradeca-2E,4E,8Etrienoic acid 4-hydroxyphenylethylamide	C ₂₂ H ₃₁ NO ₂	341	1.68	0.74	AA
25.99	2052	2E,4E-deca-2,4-dienoic acid 2-phenylethyl amide	C ₁₈ H ₂₅ NO	271	11.22	0.45	AA
26.12	2068	Deca-2E,4E-dienoic acid piperideide	C ₁₅ H ₂₃ NO	233	3.13	0.23	AA
26.30	2078	Deca-2E,4E,6Z-trienoic acid piperideide/Deca-2E,4E,6E-trienoic acid piperideide	C ₁₅ H ₂₁ NO	231	1.49	0.03	AA
26.40	2096	Deca-2E,4E,6Z,8Ztetraenoic acid piperideide/Deca-2E,4E,6E,8Ztetraenoic acid piperideide	C ₁₅ H ₁₉ NO	229	1.34	0.78	AA
26.52	2116	Tetradeca-2E,4E,12Ztriene-8,10-diynoic acid isobutylamide	C ₁₈ H ₂₃ NO	269	0.88	0.19	AA
26.67	2124	Phytol	C ₂₀ H ₄₀ O	296	0.44	0.34	D
26.87	2158	Linoleic acid ethyl ester	C ₂₀ H ₃₆ O	308	1.69	0.36	E
32.81	2200	Myristamide	C ₁₄ H ₂₉ NO	227	1.51	0.21	AA
34.68	2275	Palmitoleamide	C ₁₆ H ₃₁ NO	253	1.13	0.58	AA
35.07	2377	Oleamide	C ₁₈ H ₃₅ NO	281	17.53	0.27	AA
35.23	2399	Stearamide	C ₁₈ H ₃₇ NO	283	3.46	0.13	AA
37.75	2410	Eicosane	C ₂₀ H ₄₂	282	1.47	0.45	A
37.97	2734	Tetracosanoic acid, methyl ester	C ₂₅ H ₅₀ O	366	1.73	0.78	E
39.50	2837	Squalene	C ₃₀ H ₅₀	410	2.12	0.60	T
39.77	3172	Stigmasterol	C ₂₉ H ₄₀ O	412	8.78	0.29	S
39.99	3353	γ-Sitosterol	C ₂₉ H ₅₀ O	414	3.55	0.78	S
40.46	3370	Lupeol	C ₃₀ H ₅₀ O	426	2.63	0.97	T
		Terpenes (%)					7.52
		Alkylamides (%)					59.59
		Alkanes (%)					2.99
		Fatty acids (%)					7.51
		Esters (%)					3.42
		Sterols (%)					12.33
		Total identified components (%)					93.36

Values are means ± standard deviations (n=3). A: alkane; AA: alkylamide; D: diterpene; E: ester; FA: fatty acid; S: sterol; SA: sesquiterpene alcohol; SC: sesquiterpene hydrocarbon; SO: sesquiterpene oxide; T: triterpene; RI: retention index on DB-5-MS column relative to n-alkanes C8-C30; R_i: retention time; SE: standard error

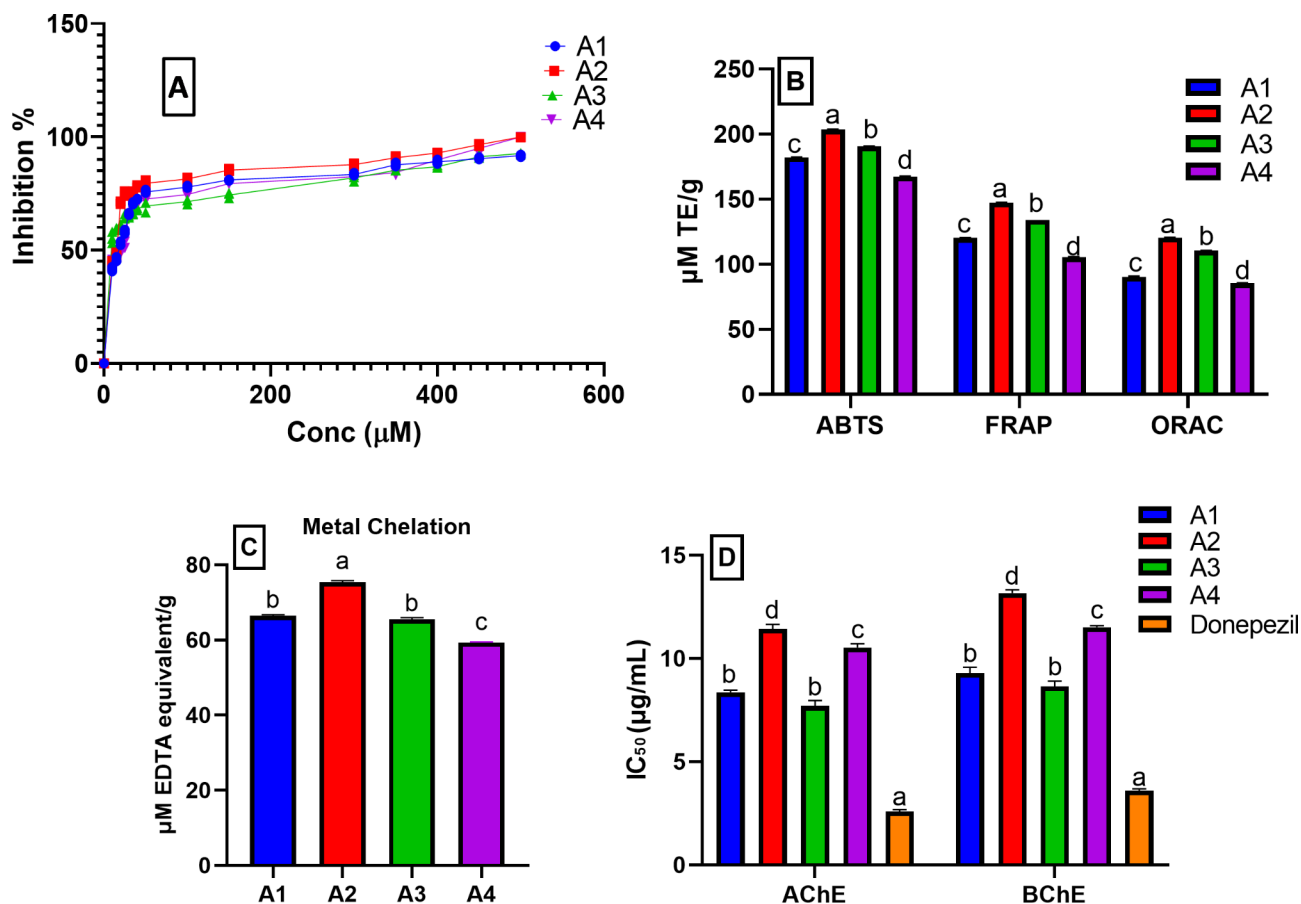


Fig. 3 Antioxidant activity using (A) DPPH represented by a line graph, (B) ABTS, FRAP, and ORAC assays, (C) metal chelating assay, and (D) anticholinergic activity (AChE and BChE) of the isolated compounds (A1–A4). μM : micromolar; TE: Trolox equivalent. Data are expressed as mean \pm standard deviation of three replicates; Different letters on the bar indicate significant differences at $P < 0.05$ with Tukey's test

(Fig. 3C) ranging from 75.36 ± 0.46 to 59.34 ± 0.19 μM EDTA equivalent/g. The results were in accordance with previous reports describing the antioxidant activity and metal chelating activity of alkylamides [54]. Moreover, the results are compatible with the previously reported antioxidant potentials of fatty amides and stigmaterol [55].

Anticholinergic activities of the isolated compound (A1–A4)

The four isolated compounds showed powerful anticholinergic activities against AChE and BChE (Fig. 3D). Among the isolated compounds, A3 and A1 showed the highest AChE inhibitory potential with IC_{50} 7.70 ± 0.26 and 8.37 ± 0.10 μM , respectively compared to the standard Donepezil (IC_{50} 2.59 ± 0.09 μM). Moreover, they were the most potent BChE inhibitors (IC_{50} 8.65 ± 0.25 and 9.29 ± 0.29 μM , respectively) relative to Donepezil (IC_{50} 3.60 ± 0.08 μM). It has been reported that alkylamides have marked AChE inhibitory activities and that is in agreement with our results [56]. It is worth noting that, the inhibitory effects of A1 and A3 were

comparable. Herein, the *in vitro* AChE and BChE inhibitory potential of oleamide (A1) was revealed for the first time.

Anti-inflammatory activities of the isolated compounds (A1–A4)

The *in vitro* inhibitory effects of the isolated compounds on the inflammatory enzymes COX-2 and 5-LOX were evaluated (Fig. 4A). The isolated compounds showed remarkable COX-2 inhibitory activities ranging from 5.11 ± 0.12 to 10.70 ± 0.15 μM compared the standard Celecoxib (IC_{50} 1.13 ± 0.08 μM). The isolated compounds exhibited also powerful 5-LOX inhibitory potentials ranging from 7.280 ± 0.27 to 12.18 ± 0.12 μM relative to the standard Zileuton (IC_{50} 5.08 ± 0.06 μM). Interestingly, A2 had the highest COX-2 and 5-LOX inhibitory activities, followed by A3 and A1, and finally, A4, which had the least effect on the tested enzymes. These results are supported by previous studies highlighting the anti-inflammatory activities of alkylamides [38], stigmaterol [57], and oleamide [58]. This study explores the anti-inflammatory activities of the isolated compounds and

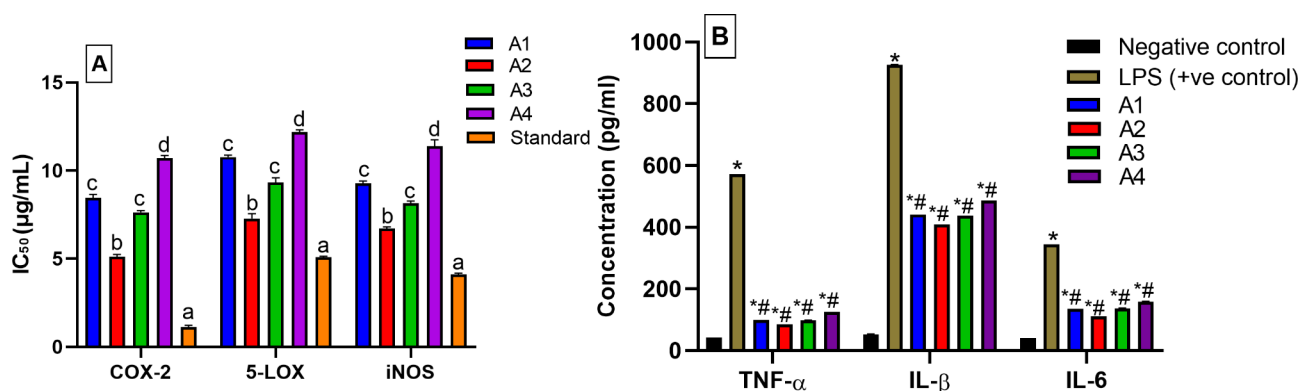


Fig. 4 (A) In vitro COX-2 and 5-LOX, as well as in LPS-induced RAW264.7 macrophages (iNOS) anti-inflammatory activities, and (B) the inhibitory effect of pro-inflammatory cytokines (TNF- α , IL-1 β , and IL-6) secretion in LPS-stimulated RAW264.7 macrophage cells of the isolated compounds (A1-A4). Different letters on the bar indicate significant differences at $P < 0.0001$. * Significant from negative control at $P < 0.0001$. # Significant from positive control at $P < 0.0001$ with Tukey's test

ascertains that they can potentially combat inflammation which results in exacerbating AD.

Effect of the isolated compounds (A1-A4) on iNOS activity in LPS-induced RAW264.7 macrophages

The isolated compounds inhibited iNOS in LPS-induced RAW264.7 macrophages (Fig. 4A), with IC₅₀ values ranging from 6.72 ± 0.08 – 11.38 ± 0.36 μ M compared to the standard drug Parthenolide (IC₅₀ = 4.10 ± 0.08 μ M). Stigmasterol (A2) was the most active (IC₅₀ 6.72 ± 0.08 μ M), followed by A3 and A1 with IC₅₀ values of 9.15 ± 0.12 μ M and 10.29 ± 0.12 μ M, respectively. While A4 appeared to be the least active and had IC₅₀ of 11.38 ± 0.36 μ M. So far, the four isolated compounds seemed to have anti-neuro-inflammatory potential fighting the most important risk factor for AD and providing a new strategy for the development of anti-AD drugs.

Effect of the isolated compounds (A1-A4) on pro-inflammatory cytokines production

The anti-inflammatory activity of the isolated compounds (A1-A4) was justified in a cell-based assay using RAW264.7 macrophages. The secretion of TNF- α , IL-1 β , and IL-6 increased after treatment with LPS alone but the co-treatment with LPS and each isolated compound significantly decreased the pro-inflammatory cytokines production ($p < 0.0001$) compared to the positive control (Fig. 4B). Depending on the current results, the four compounds are appreciated as anti-inflammatory agents with resemble effects. These results were justified by published studies showing the potential effects of oleamide [59], stigmasterol [57], and pellitorine [29]. These results report, for the first time, the promising inhibitory activity of deca-2E,4E-dienoic acid 2-phenylethylamide (A3) against the pro-inflammatory cytokines in LPS-induced RAW264.7 macrophages. Accordingly, these results suggested that the anti-inflammatory effect of MCF could be

associated with the suppression of NO production and iNOS expression through the down-regulation of TNF- α , IL-1 β , IL-6, and COX-2. Best of our knowledge, this is the first study that evaluated the combinative effects of Akarkara root-derived metabolites with anti-inflammatory, antioxidant, and anticholinesterases effects. Our results highlighted the health benefits of such a traditional remedy that possesses various meritorious properties for drug discovery. It could treat neurodegenerative diseases by different mechanisms, including alleviation of oxidative stress, inhibition of inflammatory processes, reducing plaque formation, and preventing neural cell apoptosis.

In silico studies

Molecular docking

To explore the potential anticholinergic activity of the isolated compounds; oleamide (A1) stigmasterol (A2), deca-2E,4E-dienoic acid 2-phenylethylamide (A3), and pellitorine (A4), they were tested for their inhibitory activity against AChE and BChE. The isolated compounds displayed pronounced activities against both enzymes. Consequently, a molecular docking study was performed for the mentioned compounds using AChE as a target protein to rationalize their promising inhibitory activity and to predict their plausible binding modes. A1, A2, A3, and A4 were docked into the three-dimensional X-ray crystallographic structure of AChE (PDB code: 4EY7) [60] in complex with Donepezil. The three subsites that make up the AChE active site are a peripheral anionic site (PAS), which contains Phe295, Asp74, Tyr124, and Trp286 residues, a mid-aromatic gorge, and a catalytic active site (CAS) made up of the amino acids Gly448, Glu202, Tyr337, and Trp86. Clearly, the anti-Alzheimer drug Donepezil forms water mediated hydrogen bonds with Tyr337 and Asp74 via its positively charged NH and a hydrogen bond with Phe295 through

its carbonyl moiety. Moreover, pi-stacking interactions are observed with Trp86 and Trp286 (Fig. S6). Docking setup was first validated by self-docking of the native ligand, Donepezil, into the active site of AChE. The validation results disclosed that the docking methodology is appropriate for the proposed docking study. This was supported by the fact that Donepezil coordinates and its self-docked pose were perfectly aligned displaying a root mean square deviation (RMSD) of 0.1402 Å and binding affinity (*S*) of -9.1833 Kcal mol⁻¹. Additionally, the self-docked pose was able to accomplish the same binding interactions with the essential amino acids in AChE binding site as the co-crystallized ligand (Fig. S7). Examining the top docking poses of the four tested compounds revealed that oleamide (A1) was able to achieve two hydrogen bonds with Gly120 and Trp86 in the CAS through its amide moiety. Stigmasterol (A2)

displayed a strong hydrogen bond with Glu202 in the CAS via its hydroxyl group. Some hydrogen-π interactions were also observed with the aromatic moieties of Trp286 in the PAS and Tyr341. The NH of deca-2E,4E-dienoic acid 2-phenylethylamide (A3) was engaged in water-mediated hydrogen bond with Tyr337 in the CAS in a similar mode to the co-crystallized ligand Donepezil, in addition to several hydrogen-π interactions with the aromatic moieties of Trp286 in the PAS, Tyr337, and Tyr341. The carbonyl group of pellitorine (A4) formed a hydrogen bond with Phe295 in the PAS like Donepezil and another hydrogen bond with Phe338. Besides, the docked compound showed two hydrogen-π interactions with Trp86 and one hydrogen-π interactions with Tyr337 (Fig. 5), it is worth mentioning that both amino acid residues exist in the CAS. Results of the molecular docking study (Fig. 5) of compounds A1-A4 and Donepezil in the

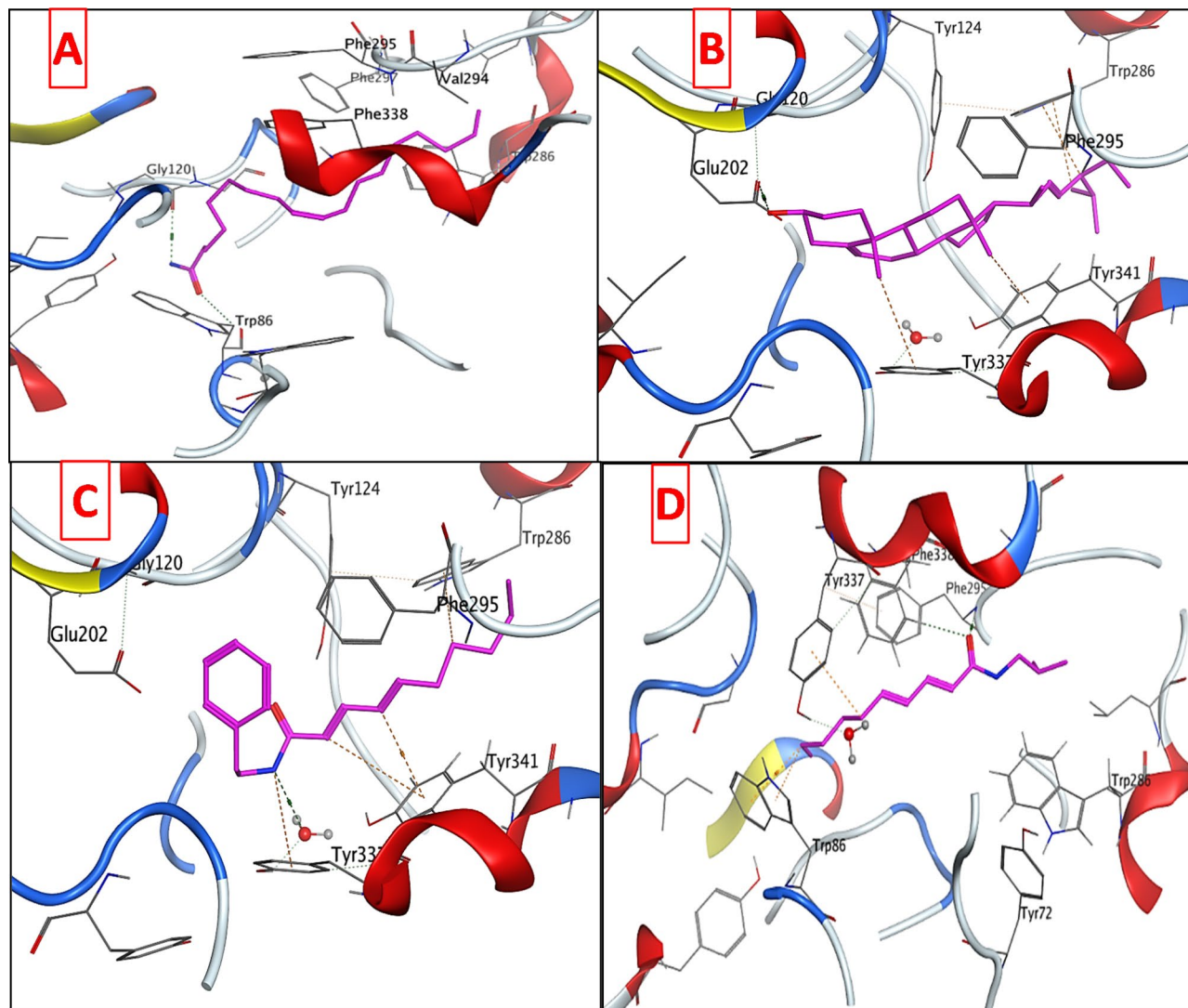


Fig. 5 3D interaction diagrams of (A) oleamide (A1), (B) stigmasterol (A2), (C) deca-2E,4E-dienoic acid 2-phenylethylamide (A3), and (D) pellitorine (A4) in AChE binding site

Table 2 Molecular docking data of the tested compounds in the AChE active site

Compound	S (Kcal mol ⁻¹)	Amino acids	Inter-acting groups	Type of interaction	Length
Oleamide (A1)	-7.2476	Trp86	C=O	H-bond	3.21
		Gly120	NH ₂	acceptor	2.86
Stigmasterol (A2)	-6.4568	Tyr337	CH ₃	H-Pi interaction	3.87
		Tyr341	CH ₃	H-Pi interaction	3.51
		Trp286	CH ₃	H-Pi interaction	3.9
		Trp286	CH	H-Pi interaction	3.44
		Glu202	OH	H-bond donor	2.84
Deca-2E,4E-dienoic acid 2-phenylethylamide (A3)	-7.2342	Tyr337	NH	H ₂ O-mediated	2.93
		Tyr337	NH	H-bond	4.28
		Tyr341	=CH	H-Pi interaction	4.54
		Tyr341	=CH	H-Pi interaction	3.72
Pellitorine (A4)	-6.6189	Trp286	CH ₂	H-Pi interaction	4.76
		Tyr337	CH ₂	H-Pi interaction	4.03
		Phe295	C=O	H-bond	3.22
		Phe338	C=O	acceptor	3.82
		Trp86	CH ₂	H-bond	3.86
		Trp86	CH ₂	acceptor	4.29
Donepezil	-9.1833			H-Pi interaction	
		Asp74	NH ⁺	H ₂ O-mediated	2.88
		Tyr337	NH ⁺	H-bond	2.88
		Tyr341	CH ₂	H ₂ O-mediated	3.64
		Phe295	C=O	H-bond	3.28
		Trp286	Phenyl	H-Pi interaction	3.80
Trp86	Phenyl	H-bond	3.94		
			acceptor		
			Pi-Pi interaction		
			Pi-Pi interaction		

vicinity of AChE were recorded in Table 2. Overall, the docked compounds fit well in the active site of AChE and were able to occupy the catalytic active site and peripheral anionic site of the enzyme, achieving comparable docking scores to that of the native ligand. Compounds A1 and A3 displayed the highest docking scores (binding energies) reaching about (79%) of that of Donepezil. These results are well correlated with the respective *in vitro* assessment of the anticholinergic activity of the isolated compounds.

The isolated compounds were also examined for their potential anti-inflammatory activity by performing enzyme inhibitory assay against COX-2, 5-LOX, and iNOS. The most promising results were attained against COX-2. Thus, the four tested compounds were docked in the vicinity of COX-2 binding site to justify their potency. The three-dimensional X-ray crystallographic structure of COX-2 (PDB code: 3LN1) [61] in complex with the Celecoxib was retrieved from the protein data bank. It is worth mentioning that the amino group of Celecoxib can donate three hydrogen bonding interactions with Ser339,

Table 3 Molecular docking data of the tested compounds in COX-2 active site

Compound	S (Kcal mol ⁻¹)	Amino acids	Inter-acting groups	Type of interaction	Length
Oleamide (A1)	-11.7343	Ser339	NH ₂	H-bond donor	2.96
		Gln178	NH ₂	H-bond donor	3.03
Stigmasterol (A2)	-14.6288	Ser516	OH	H-bond donor	2.61
Deca-2E,4E-dienoic acid 2-phenylethylamide (A3)	-11.4957	Leu338	NH	H-bond donor	2.91
		Thr79	Phenyl	H-Pi interaction	3.86
Pellitorine (A4)	-10.8175	Ser516	C=O	H-bond acceptor	2.68
Celecoxib	-9.6345	Ser339	NH ₂	H-bond donor	2.93
		Leu338	NH ₂	H-bond donor	3.04
		Gln178	NH ₂	H-bond donor	3.06
		Arg499	SO ₂	H-bond acceptor	3.54

Leu338, and Gln178 (Fig. S8). Additionally, another hydrogen bond is observed between the sulfonyl group and Arg499. Moreover, the validation outcomes demonstrated that the co-crystallized ligand could dock properly in COX-2 active site with root mean square deviation (RMSD) of 0.0903 Å and docking score (S) of -9.6345 Kcal mol⁻¹ (Fig. S9).

Investigation of the docking data showed that the four docked compounds were able to achieve higher binding scores compared to the native ligand Celecoxib (Table 3). Oleamide (A1) donated two hydrogen bonding interactions to Ser339 and Gln178 similar to Celecoxib. Stigmasterol (A2) and pellitorine (A4) attained hydrogen bonds with Ser516 via their hydroxyl and carbonyl moieties, respectively, which could enhance the COX-2 inhibitory activity [62]. Moreover, deca-2E,4E-dienoic acid 2-phenylethylamide (A3) exhibited nearly similar orientation in the binding site of COX-2 through one hydrogen bonding interaction with leu338 and an arene-π interaction with Thr79. The results are represented in Fig. 6 and Table 3.

The anti-inflammatory capacity of the Akarkara root against cognitive deficits and neurodegenerative conditions that are characteristics of AD, was assumed to be associated mainly with its nonpolar composition (Fig. 2). Thus, the interactions of the compounds isolated from the MCF with COX-2 receptor were investigated *in silico* via molecular docking. The four compounds docked within the COX-2 receptor gave binding energy values ranging from 10.8175 Kcal mol⁻¹(A2) to 14.6288 kcal mol⁻¹ (A4). Thus, the remarkable binding affinities of the isolated compounds and their promising binding modes and interactions in the vicinity of COX-2 could justify the significant *in vitro* inhibitory activity of the investigated

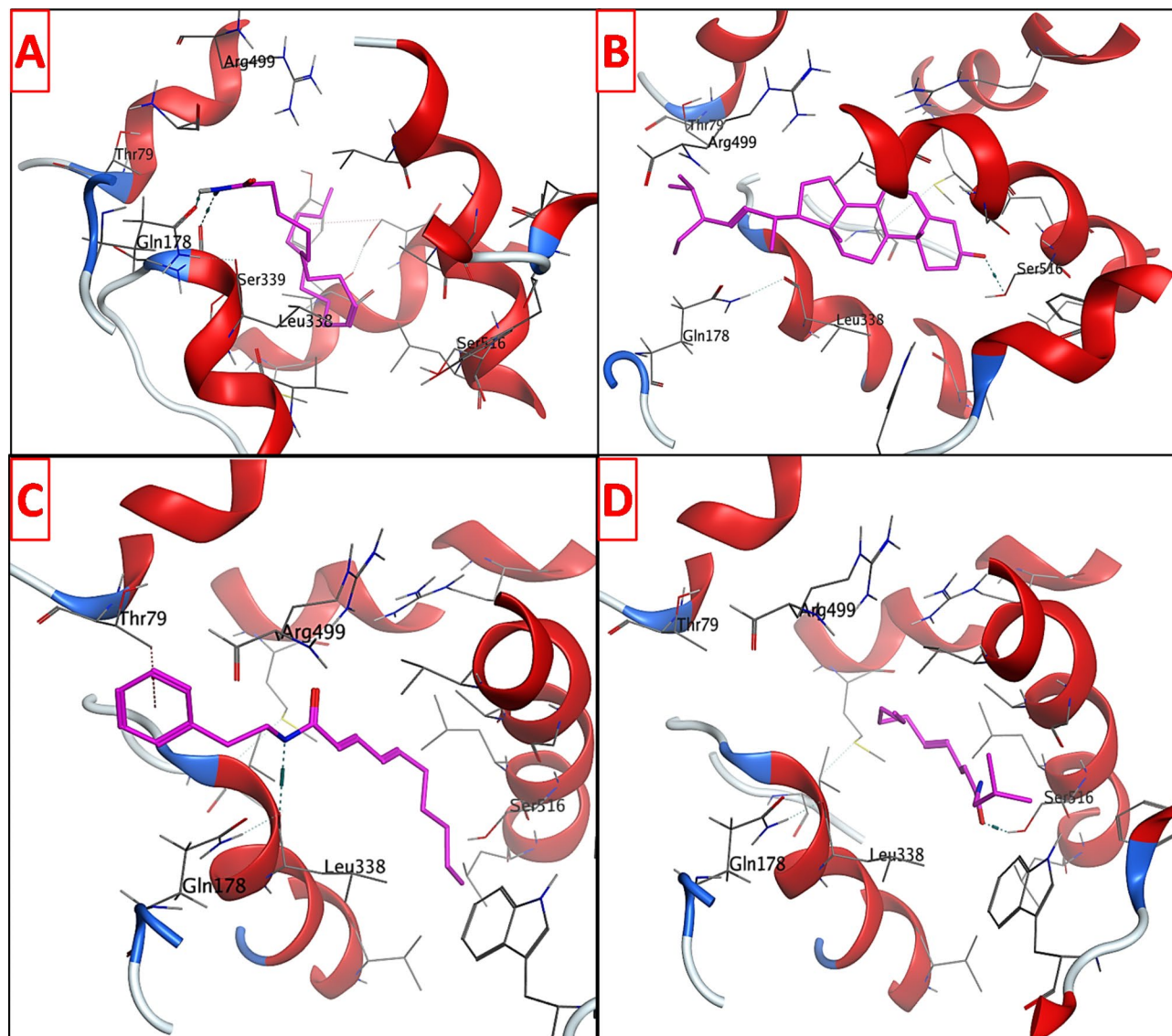


Fig. 6 3D interaction diagrams of (A) oleamide (A1), (B) stigmasterol (A2), (C) deca-2E,4E-dienoic acid 2-phenylethylamide (A3), and (D) pellitorine (A4) in COX-2 binding site

parent extract and its fractions in comparison to Celecoxib, supporting the possibility of a synergistic anti-inflammatory effect exerted by the isolated compounds. Finally, the current findings support the notion that some plants have better prospects as neurodegenerative protectors due to their potential anticholinergic and anti-inflammatory properties.

***In silico* ADME profile and BBB permeability prediction**

The pharmacokinetics, physicochemical, and drug likeness properties of the four isolated compounds were predicted using the free accessible web server Swiss ADME (<http://www.swissadme.ch/index.php>). The outcomes of Swiss ADME prediction (Table 4) demonstrated that the examined compounds accomplished a predicted log Po/w

value in the range of 3.64–6.98 and revealed no alerts for Pan Assay Interfering Substances (PAINS). Besides, three out of the four compounds were moderately water soluble, BBB permeable, and possessed high GIT absorption (for the boiled egg chart of the tested compounds see supporting materials, Fig. S10). All the tested compounds were not P-glycoprotein substrates. The Lipinski rule of five [63] and other models were used to determine the bioavailability scores. The molecular interactions involving cytochromes P450 isomers (CYP) were anticipated. Moreover, the oral bioavailability radar charts of the examined compounds displayed that they had good anticipated oral bioavailability as well as favorable pharmacokinetic features as depicted in Fig. 7.

Table 4 ADME properties of the isolated compounds predicted using SwissADME web server

Property	Oleamide (A1)	Stigmasterol (A2)	Deca-2E,4E-dienoic acid 2-phenylethylamide (A3)	Pellitorine (A4)
MW	281.48	412.69	271.4	223.35
Consensus LogPo/w	5.29	6.98	4.29	3.64
Log S (ESOL)	Moderately soluble	Poorly soluble	Moderately soluble	Soluble
#Rotatable bonds	15	5	10	9
#H-bond acceptors	1	1	1	1
#H-bond donors	1	1	1	1
MR	91.07	132.75	86.34	71.47
TPSA	43.09	20.23	29.10	29.10
Lipinski violations	1	1	0	0
Ghose violations	0	3	0	0
Veber violations	1	0	0	0
Egan violations	0	1	0	0
Muegge violations	1	2	1	0
Bioavailability score	0.55	0.55	0.55	0.55
PAINS alerts	0	0	0	0
Brenk alerts	1	1	2	2
Leadlikeness violations	2	2	2	3
GI absorption	High	Low	High	High
BBB permeant	Yes	No	Yes	Yes
P-gp substrate	No	No	No	No
CYP1A2 inhibitor	Yes	No	Yes	Yes
CYP2C19 inhibitor	No	No	Yes	No
CYP2C9 inhibitor	Yes	Yes	Yes	No
CYP2D6 inhibitor	No	No	No	No
CYP3A4 inhibitor	No	No	No	No

BBB: Blood-brain barrier; GI: Gastrointestinal; MR: Molar refractivity; P-gp: P-glycoprotein; PAINS: Pan Assay Interfering Substances; TPSA: Topological polar surface area

Crossing the blood-brain barrier is a necessity for drugs targeting the CNS. The inability of therapeutic molecules to penetrate the BBB is a key obstacle for CNS drug candidates and needs to be addressed quickly in the drug

development process. Predicting the BBB permeability of new CNS drugs is therefore crucial. Accordingly, the BBB distribution for our candidates was additionally assessed using the web server pkCSM (<http://biosig.unimelb.edu.au/pkcsm/prediction>) in comparison with Donepezil as a reference drug [64]. The BBB permeability (blood-brain barrier permeability log BB) and CNS permeability (calculated using the blood-brain permeability surface area product log PS) are two *in silico* parameters provided by the pkCSM server. The first foretells a compound's capability to cross the BBB. The second parameter does not account for the effects of the systemic distribution and is associated with the direct assessment of brain-blood permeability. Regarding the BBB permeability, all the tested compounds are readily able to cross the BBB, with values ranging from 0.811 to -0.397 in comparison with Donepezil (0.157). Considering the CNS permeability, the assessed compounds have high ability to penetrate the CNS with values ranging from 1.596 to -1.651 in comparison with Donepezil (-1.464). The calculated results are illustrated in Table 5.

Molecular dynamic and system stability

A molecular dynamic simulation was carried out to predict the performance of the isolated compounds upon binding to the active site of protein as well as their interaction and stability through the simulation [65, 66]. The validation of system stability is essential to trace disrupted motions and avoid artifacts that may develop during the simulation. This study assessed Root-Mean-Square Deviation (RMSD) to measure the systems' stability during the 60 ns simulations. The recorded average RMSD values for the entire frames of the systems were $1.52 \pm 0.22 \text{ \AA}$, and $1.37 \pm 0.18 \text{ \AA}$, for apo-AChE protein, and oleamide-AChE complex systems (Fig. 8A), and $1.80 \pm 0.18 \text{ \AA}$, $1.69 \pm 0.21 \text{ \AA}$, for COX-Apo, COX-stigmasterol complex, respectively (Fig. 9A).

During MD simulation, assessing protein structural flexibility upon ligand binding is critical for examining residue behavior and their connection with the ligand [67]. Protein residues fluctuations were evaluated using Root-Mean-Square Fluctuation (RMSF) algorithm to evaluate the effect of inhibitor binding towards the respective targets over 60 ns simulations. The recorded average RMSF values for the entire frames of the systems were $1.02 \pm 0.60 \text{ \AA}$, and $0.94 \pm 0.54 \text{ \AA}$, for apo-AChE protein, and oleamide-AChE complex systems (Fig. 8B), and $1.16 \pm 0.60 \text{ \AA}$, $1.11 \pm 0.53 \text{ \AA}$, for COX-Apo, COX-stigmasterol complex, respectively (Fig. 9B). These values revealed that the oleamide-, and stigmasterol-bound to protein complex systems had a lower residue fluctuation than the other systems.

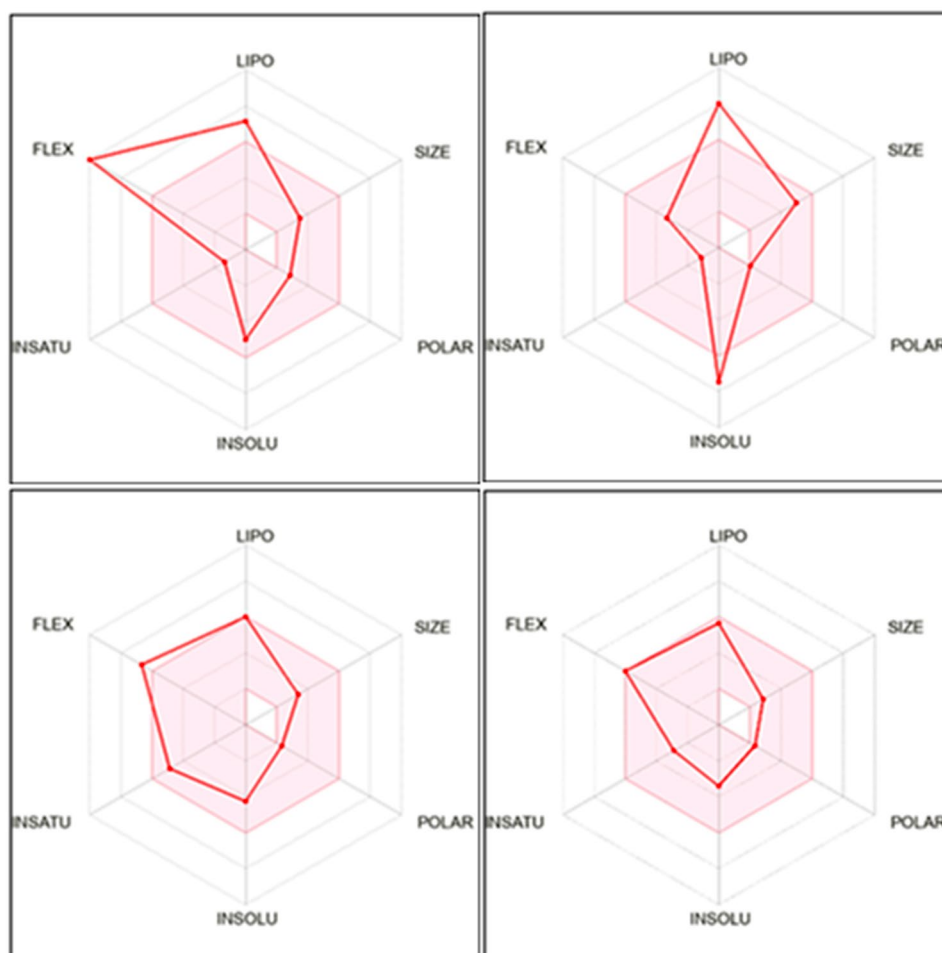


Fig. 7 Bioavailability radar chart of the isolated compounds; oleamide (**A**), stigmasterol (**A2**), deca-2E,4E-dienoic acid 2-phenylethylamide (**A3**), and pellitorine (**A4**), respectively. The pink zone signifies the range of the optimal property values for oral bioavailability and the red line is the compounds' predicted properties. Saturation (INSATU), size (SIZE), polarity (POLAR), solubility (INSOLU), lipophilicity (LIPO), and flexibility (FLEX)

Table 5 The central nervous system (CNS) distribution values of the isolated compounds calculated using pkCSM web server

Compound	Distribution	
	BBB permeability (log BB) ^a	CNS permeability (log PS) ^b
Oleamide (A1)	-0.397	-1.651
Stigmasterol (A2)	0.811	-1.033
Deca-2E,4E-dienoic acid 2-phenylethylamide (A3)	0.603	-0.976
Pellitorine (A4)	0.633	1.596
Donepezil	0.157	-1.464

^alog BB should be >0.3 and not less than -1 for a compound to readily cross the BBB

^blog PS should be > -2 and not less than -3 for a compound to penetrate the CNS

The radius of gyration (R_g) is an indicator of protein structure compactness and stability during the simulation [68]. The recorded average RMSF values for the entire frames of the systems were $23.08 \pm 0.08 \text{ \AA}$, and $23.07 \pm 0.06 \text{ \AA}$, for apo-AChE protein, and oleamide-AChE complex (Fig. 8C), and $24.33 \pm 0.092 \text{ \AA}$, $24.05 \pm 0.07 \text{ \AA}$, for COX-Apo, COX-stigmasterol complex, respectively (Fig. 9C). It was found that R_g of ligand-bonded protein exhibited a lower rigid structure than Apo-protein.

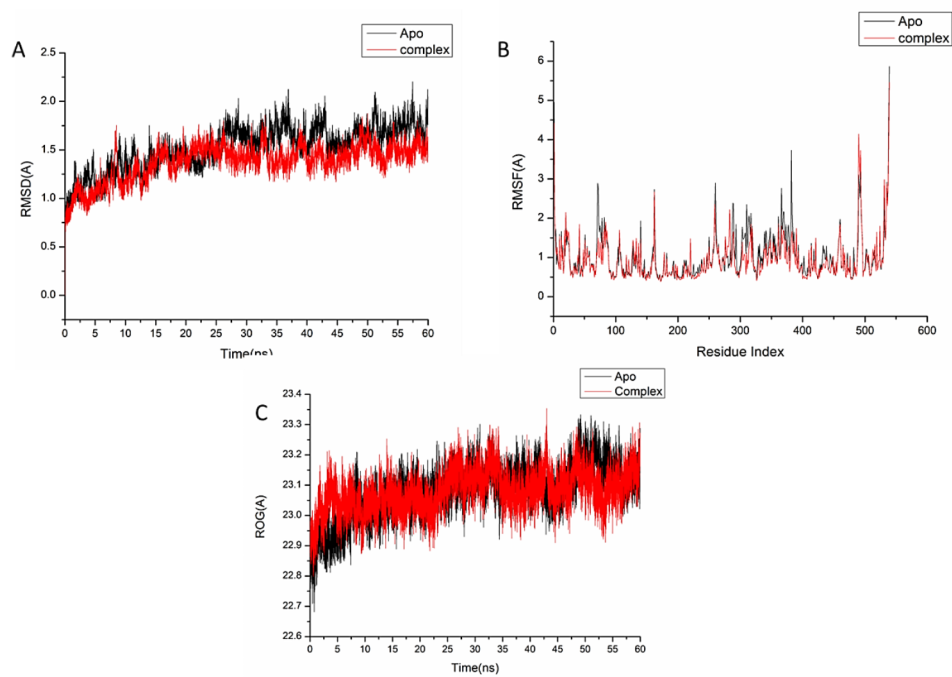


Fig. 8 (A) RMSD of Ca atoms of the protein backbone atoms. (B) RMSF of each residue of the protein backbone Ca atoms. (C) RoG of Ca atoms of protein residues of the backbone atoms relative (black) to the starting minimized over 60 ns for the acetylcholinesterase receptor (AChE) receptor enzymes protein with oleamide (red)

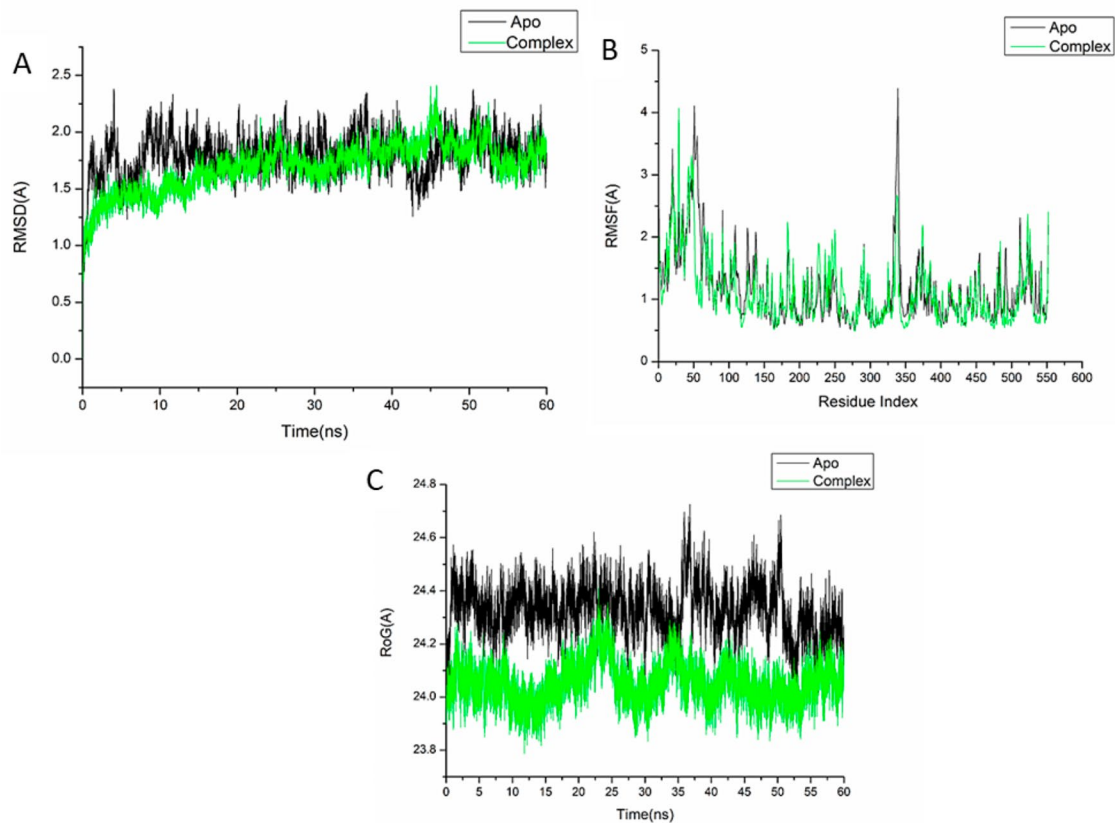


Fig. 9 (A) RMSD of Ca atoms of the protein backbone atoms. (B) RMSF of each residue of the protein backbone Ca atoms (C) RoG of Ca atoms of protein residues of the backbone atoms relative (black) to the starting minimized over 60 ns for the cyclooxygenase-2 receptor enzymes protein with stigmasterol (green)

Conclusion

This research shed light on *A. pyrethrum* as a multifunctional anti-Alzheimer drug in a first report. We can use the chemical profile of the methylene chloride fraction of *A. pyrethrum* L. roots obtained by GC-MS as a marker for its identification through elucidation of the main active constituents and establishing their proportions and the characteristic ratios between them. The isolated compounds showed potential antioxidant, anticholinergic, and anti-inflammatory activities. In this respect, the molecular docking and dynamic simulations with the key cholinergic (AChE) and inflammatory (COX-2) enzymes recommended these compounds as valuable multifactorial anti-Alzheimer drugs. Thus, further in vivo and clinical studies on *A. pyrethrum* and its isolated compounds are warranted to clarify their therapeutic potential as drug candidates targeting AD for clinical use.

Abbreviations

ABTS	2,2'-azino-di(3-ethylbenzthiazoline-6-sulfonic acid)
AChE	Acetylcholinesterase
AD	Alzheimer's disease
BChE	Butyrylcholinesterase
COX	Cyclooxygenase
DPPH	2,2-diphenyl-1-picrylhydrazyl
DW	Dried weight
FRAP	Ferric reducing antioxidant power
IC ₅₀	Half maximal inhibitory concentration
IL	Interleukin
LOX	Lipoxygenase
iNOS	Inducible nitric oxide synthase
BF	Butanol fraction
MCF	Methylene chloride fraction
ME	Methanolic extract
ORAC	Oxygen radical absorbance capacity
TE,	Trolox equivalent
TNF- α	Tumor necrosis factor alpha

Supplementary Information

The online version contains supplementary material available at <https://doi.org/10.1186/s12906-023-04210-6>.

Supplementary Material 1

Authors' contributions

R.M.I. and N.E.M.: isolation and identification of pure compounds. P.M.A.: set the main idea of the manuscript. G.F.E.: carrying molecular docking of the isolated compounds. A.A.E.: carrying molecular dynamics simulation of the isolated compounds. All the authors: designing of the experiment; writing and revising the manuscript. All authors have read and agreed to the published version of the manuscript.

Funding

This research received no external funding. Open access funding provided by The Science, Technology & Innovation Funding Authority (STDF) in cooperation with The Egyptian Knowledge Bank (EKB).

Data Availability

All data generated or analyzed during this study are included in this published article and its supplementary information file.

Declarations

Ethics approval and consent to participate

This article does not contain any studies with human participants or animals performed by any of the authors.

Consent for publication

Not applicable.

Competing interests

The authors declare no competing interests.

Author details

¹Pharmacognosy Department, Faculty of Pharmacy, Cairo University, Kasr El-Ainy Street, Cairo 11562, Egypt

²Department of Pharmaceutical Chemistry, Faculty of Pharmacy, Cairo University, Kasr El-Aini Street, Cairo 11562, Egypt

³Natural and Microbial Products Department, National Research Center (NRC), Dokki, Giza 12622, Egypt

Received: 18 July 2023 / Accepted: 9 October 2023

Published online: 17 November 2023

References

1. WHO. Global action plan on the public health response to dementia 2017–2025. 2017.
2. Prince MJ, Wimo A, Guerchet MM et al. World Alzheimer Report 2015-The Global Impact of Dementia: An analysis of prevalence, incidence, cost and trends. 2015.
3. Perry SW, Norman JP, Barbieri J, et al. Mitochondrial membrane potential probes and the proton gradient: a practical usage guide. *Biotechniques*. 2011;50:98–115. <https://doi.org/10.2144/000113610>.
4. Matough FA, Budin SB, Hamid ZA, et al. The role of oxidative stress and antioxidants in diabetic Complications. *Sultan Qaboos Univ Med J*. 2012;12:5. <https://doi.org/10.12816/0003082>.
5. Ames B, Gold L. Animal cancer tests and cancer prevention. *J Natl Cancer Inst Monogr*. 1992; 125–32.
6. Guyton K, Kensler T. Oxidative mechanisms in carcinogenesis. *Br Med Bull*. 1993;49:523–44. <https://doi.org/10.1093/oxfordjournals.bmb.a072628>.
7. Azeem MNA, Ahmed OM, Shaban M, et al. In vitro antioxidant, anticancer, anti-inflammatory, anti-diabetic and anti-alzheimer potentials of innovative macroalgae bio-capped silver nanoparticles. *Environ Sci Pollut Res*. 2022;29:59930–47. <https://doi.org/10.1007/s11356-022-20039-x>.
8. Wang Z-M, Cai P, Liu Q-H, et al. Rational modification of donepezil as multi-functional acetylcholinesterase inhibitors for the treatment of Alzheimer's Disease. *Eur J Med Chem*. 2016;123:282–97. <https://doi.org/10.1016/j.ejmech.2016.07.052>.
9. Colovic MB, Krstic DZ, Lazarevic-Pasti TD, et al. Acetylcholinesterase inhibitors: pharmacology and toxicology. *Curr Neuropharmacol*. 2013;11:315–35.
10. Bagyinszky E, Van Giau V, Shim K, et al. Role of inflammatory molecules in the Alzheimer's Disease progression and diagnosis. *J Neurol Sci*. 2017;376:242–54. <https://doi.org/10.1016/j.jns.2017.03.031>.
11. Sharma V, Thakur M, Chauhan NS, et al. Evaluation of the anabolic, aphrodisiac and reproductive activity of *Anacyclus pyrethrum* DC in male rats. *Sci Pharm*. 2009;77:97–110. <https://doi.org/10.3797/scipharm.0808-14>.
12. Prajapati ND, Purohit S, Sharma AK et al. A handbook of medicinal plants: A complete source book. In: A handbook of medicinal plants: a complete source book. 2003: 554–554.
13. Rani S, Kaushik V, Saini V et al. Biological studies of *Anacyclus pyrethrum*. *Am J Pharm Res*. 2013; 3.
14. Jawhari FZ, El Moussaoui A, Imtara H, et al. Evaluation of the acute toxicity of the extracts of *Anacyclus pyrethrum* var. *Pyrethrum* (L.) and *Anacyclus pyrethrum* var. *Depressus* Maire in Swiss mice. *Vet World*. 2021;14:457. <https://doi.org/10.14202/vetworld.2021.457-467>.
15. Sharma V, Boonen J, Spiegeleer BD, et al. Androgenic and spermatogenic activity of alkylamide-rich ethanol solution extract of *Anacyclus pyrethrum* DC. *Phytother Res*. 2013;27:99–106. <https://doi.org/10.1002/ptr.4697>.

16. Wilson E, Rajamanickam G, Vyas N, et al. Herbs used in siddha medicine for arthritis—a review. *Indian J Tradit Knowl*. 2007;6:678–86.
17. Boonen J, Sharma V, Dixit VK, et al. LC-MS N-alkylamide profiling of an ethanolic *Anacyclus pyrethrum* root extract. *Planta Med*. 2012;1787–95. <https://doi.org/10.1055/s-0032-1315371>.
18. Elazzouzi H, Fadili K, Cherrat A, et al. Phytochemistry, Biological and pharmacological activities of the *Anacyclus pyrethrum* (L.) lag: a systematic review. *Plants*. 2022;11:2578. <https://doi.org/10.3390/plants11192578>.
19. Usmani A, Khushtar M, Arif M, et al. Pharmacognostic and phytopharmacology study of *Anacyclus pyrethrum*: an insight. *J Appl Pharm Sci*. 2016;6:144–50.
20. Mahdy NE, Abdel-Baki PM, El-Rashedy AA, et al. Modulatory Effect of *Pyrus pyrifolia* Fruit and its phenolics on key enzymes against metabolic syndrome: Bioassay-Guided Approach, HPLC Analysis, and in Silico Study. *Plant Foods Hum Nutr (Dordrecht Netherlands)*. 2023. <https://doi.org/10.1007/s11130-023-01069-3>.
21. Manouze H, Bouchatta O, Gadhi AC, et al. Anti-inflammatory, antinociceptive, and antioxidant activities of methanol and aqueous extracts of *Anacyclus pyrethrum* roots. *Front Pharmacol*. 2017;8:598. <https://doi.org/10.3389/fphar.2017.00598>.
22. Kalim MD, Bhattacharyya D, Banerjee A, et al. Oxidative DNA damage preventive activity and antioxidant potential of plants used in Unani system of medicine. *BMC Complement Altern Med*. 2010;10:1–11. <https://doi.org/10.1186/1472-6882-10-77>.
23. Sujith K, Darwin CR, Suba V. Antioxidant activity of ethanolic root extract of *Anacyclus pyrethrum*. *Int Res J Pharm*. 2011;2:2109.
24. Pahuja M, Mehla J, Reeta K, et al. Effect of *Anacyclus pyrethrum* on pentylenetetrazole-induced kindling, spatial memory, oxidative stress and rho-kinase II expression in mice. *Neurochem Res*. 2013;38:547–56.
25. Kerboua KA, Benosmane L, Namoune S, et al. Anti-inflammatory and antioxidant activity of the hot water-soluble polysaccharides from *Anacyclus pyrethrum* (L.) lag. *Roots*. *J Ethnopharmacol*. 2021;281:114491. <https://doi.org/10.1016/j.jep.2021.114491>.
26. Tyagi S, Mansoori MH, Singh NK, et al. Antidiabetic effect of *Anacyclus pyrethrum* DC in alloxan induced diabetic rats. *Eur J Biol Sci*. 2011;3:117–20.
27. Carvajal FJ, Inestrosa NC. Interactions of AChE with A β aggregates in Alzheimer's brain: therapeutic relevance of IDN 5706. *Front Mol Neurosci*. 2011;4:19. <https://doi.org/10.3389/fnmol.2011.00019>.
28. Mahnashi MH, Alshehri OM. Isolation. In *Vitro* and in *Silico* Anti-alzheimer and anti-inflammatory studies on phytosteroids from Aerial Parts of *Fragaria x Ananassa Duch*. *Biomolecules*. 2022;12:1430. <https://doi.org/10.3390/biom12101430>.
29. Wang Q, Liang J, Stephen Brennan C, et al. Anti-inflammatory effect of alkaloids extracted from *Dendrobium aphyllum* on macrophage RAW 264.7 cells through NO production and reduced IL-1, IL-6, TNF- α and PGE2 expression. *Int J Food Sci Technol*. 2020;55:1255–64. <https://doi.org/10.1111/ijfs.14404>.
30. Sabry MM, Abdel-Rahman RF, Fayed HM, et al. Impact of *Eucalyptus maculata* hook resin exudate constituents on reducing COX-2 gene expression: In-vivo anti-inflammatory, molecular docking and dynamics studies. *J Ethnopharmacol*. 2023;116631. <https://doi.org/10.1016/j.jep.2023.116631>.
31. Honda T, Kabashima K, Kunisawa J. Exploring the roles of prostanoids, leukotriens, and dietary fatty acids in cutaneous inflammatory Diseases: insights from pharmacological and genetic approaches. *Immunol Rev*. 2023. <https://doi.org/10.1111/immr.13193>.
32. Sujith K, Darwin R, Suba V. Toxicological evaluation of ethanolic extract of *Anacyclus pyrethrum* in albino wistar rats. *Asian Pac J Trop Dis*. 2012;2:437–41. [https://doi.org/10.1016/S2222-1808\(12\)60096-6](https://doi.org/10.1016/S2222-1808(12)60096-6).
33. Patocka J. Biologically active pentacyclic triterpenes and their current medicine signification. *J Appl Biomed*. 2003;1:7–12. <https://doi.org/10.32725/jab.2003.002>.
34. Fernandez M, Watson P, Breuil C. Gas chromatography–mass spectrometry method for the simultaneous determination of wood extractive compounds in quaking aspen. *J Chromatogr A*. 2001;922:225–33. [https://doi.org/10.1016/S0021-9673\(01\)00948-7](https://doi.org/10.1016/S0021-9673(01)00948-7).
35. Lopez KS, Marques AM, Moreira DDL, et al. Local anesthetic activity from extracts, fractions and pure compounds from the roots of *Ottonia Anisum Spreng* (Piperaceae). *An Acad Bras Cienc*. 2016;88:2229–37. <https://doi.org/10.1590/0001-3765201620150821>.
36. Canli K, Yetgin A, Akata I, et al. Antimicrobial activity and chemical composition screening of *Anacyclus pyrethrum* root. *Indian J Pharm Educ Res*. 2017. <https://doi.org/10.5530/ijper.51.3s.22>.
37. Wahab AT, Shaikh M, Naqeeb U, et al. Study of *Anacyclus pyrethrum* lag. Root Extract against *Aedes aegypti* Linn. Larvae: potential Vector Control for Dengue viral Fever. *Rec Nat Prod*. 2021;15:486. <https://doi.org/10.25135/rnp.404.2304.2761>.
38. Jawhari FZ, El Moussaoui A, Bourhia M, et al. *Anacyclus pyrethrum* (L.): Chemical composition, analgesic, anti-inflammatory, and wound healing properties. *Molecules*. 2020;25:5469. <https://doi.org/10.3390/molecules25225469>.
39. Jawhari FZ, Moussaoui AE, Bourhia M, et al. *Anacyclus pyrethrum* var. *Pyrethrum* (L.) and *Anacyclus pyrethrum* var. *Depressus* (Ball) Maire: correlation between total phenolic and flavonoid contents with antioxidant and antimicrobial activities of chemically characterized extracts. *Plants*. 2021;10:149. <https://doi.org/10.3390/plants10010149>.
40. Yousef BA, Awad Z, Adam S, et al. Assessment of Anticonvulsant activities of Petroleum Ether Extract of *Anacyclus pyrethrum* roots on experimental rats. *Pharm Biomed Res*. 2021;7:47–54. <https://doi.org/10.18502/pbr.v7i1.7356>.
41. Elufioye TO, Habtemariam S, Adejare A. Chemistry and pharmacology of alkylamides from natural origin. *Rev Bras Farmacogn*. 2020;30:622–40. <https://doi.org/10.1007/s43450-020-00095-5>.
42. Lai Shi Min S, Liew SY, Chear NJY, et al. Plant terpenoids as the promising source of cholinesterase inhibitors for anti-AD therapy. *Biology*. 2022;11:307. <https://doi.org/10.3390/biology11020307>.
43. Rao RV, Descamps O, John V, et al. Ayurvedic medicinal plants for Alzheimer's Disease: a review. *Alz Res Therapy*. 2012;4:1–9. <https://doi.org/10.1186/alzrt125>.
44. Ruzskowski P, Bobkiewicz-Kozłowska T. Natural triterpenoids and their derivatives with pharmacological activity against neurodegenerative disorders. *Mini-Rev Org Chem*. 2014;11:307–15. <https://doi.org/10.2174/1570193X1103140915111559>.
45. Miranda RS, de Jesus BSM, da Silva Luiz SR, et al. Anti-inflammatory activity of natural triterpenes—An overview from 2006 to 2021. *Phytother Res*. 2022;36:1459–506. <https://doi.org/10.1002/ptr.7359>.
46. Niaz K, Nawaz MA, Pervez S, et al. Total scale analysis of organic acids and their role to mitigate Alzheimer's Disease. *S Afr J Bot*. 2022;144:437–47. <https://doi.org/10.1016/j.sajb.2021.09.020>.
47. Devassy JG, Leng S, Gabbs M, et al. Omega-3 polyunsaturated fatty acids and oxylipins in neuroinflammation and management of Alzheimer Disease. *Adv Nutr*. 2016;7:905–16. <https://doi.org/10.3945/an.116.012187>.
48. Román G, Jackson R, Gadhia R, et al. Mediterranean diet: the role of long-chain ω -3 fatty acids in fish; polyphenols in fruits, vegetables, cereals, coffee, tea, cacao and wine; probiotics and vitamins in prevention of Stroke, age-related cognitive decline, and Alzheimer Disease. *Rev Neurol*. 2019;175:724–41. <https://doi.org/10.1016/j.neuro.2019.08.005>.
49. Ingolfsdóttir K, Gissurarson S, Nenninger A, et al. Biologically active alkamide from the lichen *Stereocaulon Alpinum*. *Phytomedicine*. 1997;4:331–4. [https://doi.org/10.1016/S0944-7113\(97\)80042-6](https://doi.org/10.1016/S0944-7113(97)80042-6).
50. Chaturvedula VSP, Prakash I. Isolation of Stigmasterol and ?-Sitosterol from the dichloromethane extract of *Rubus Suavisissimus*. *Int Curr Pharm J*. 2012;1:239–42. <https://doi.org/10.3329/icpj.v1i9.11613>.
51. Althaus JB, Malyszec K, Kaiser M, et al. Alkamide from *Anacyclus Pyrethrum* L. and their in vitro antiprotozoal activity. *Molecules*. 2017;22:796. <https://doi.org/10.3390/molecules22050796>.
52. Hamimed S, Boulebdia N, Laouer H et al. Bioactivity-guided isolation of alkamides from a cytotoxic fraction of the ethyl acetate extract of (L.) DC. Roots. *Current issues in Pharmacy and Medical sciences*. 2018; 31: 180–5. <https://doi.org/10.1515/cipms-2018-0033>.
53. Ibrahim RM, Mahdy NE, Abdel-Baki PM, et al. Chemical characterization, in vitro and in vivo evaluation of Chitosan-Aloe marlothii gel loaded nanoparticles on acetaminophen-induced hepatitis in mice. *South Afr J Bot*. 2023;157:1–9. <https://doi.org/10.1016/j.sajb.2023.03.044>.
54. Wichur T, Więckowska A, Więckowski K, et al. 1-Benzylpyrrolidine-3-amine-based BuChE inhibitors with anti-aggregating, antioxidant and metal-chelating properties as multifunctional agents against Alzheimer's Disease. *Eur J Med Chem*. 2020;187:111916. <https://doi.org/10.1016/j.ejmech.2019.111916>.
55. Radman S, Čížmek L, Babić S, et al. Bioprospecting of less-polar fractions of *Ericaria crinita* and *ericaria amentacea*: developmental toxicity and antioxidant activity. *Mar Drugs*. 2022;20:57. <https://doi.org/10.3390/md20010057>.
56. Akbar S, Akbar S, *Anacyclus pyrethrum*. (L.) Lag (Asteraceae/Compositae) (Syns.: *A. depressus* Ball; *A. freynii* Willk; *A. officinarum* Hayne; *Anthemis pyrethrum* L.). *Handbook of 200 Medicinal Plants: A Comprehensive Review of Their Traditional Medical Uses and Scientific Justifications*. 2020; 261–265. https://doi.org/10.1007/978-3-030-16807-0_25.

57. Yuan L, Zhang F, Shen M, et al. Phytosterols suppress phagocytosis and inhibit inflammatory mediators via ERK pathway on LPS-triggered inflammatory responses in RAW264. 7 macrophages and the correlation with their structure. *Foods*. 2019;8:582. <https://doi.org/10.3390/foods8110582>.
58. Shakour ZTA, Radwa H, Elshamy AI, et al. Dissection of *Moringa oleifera* leaf metabolome in context of its different extracts, origin and in relationship to its biological effects as analysed using molecular networking and chemometrics. *Food Chem*. 2023;399:133948. <https://doi.org/10.1016/j.foodchem.2022.133948>.
59. Moon S-M, Lee SA, Hong JH, et al. Oleamide suppresses inflammatory responses in LPS-induced RAW264. 7 murine macrophages and alleviates paw edema in a carrageenan-induced inflammatory rat model. *Int Immunopharmacol*. 2018;56:179–85. <https://doi.org/10.1016/j.intimp.2018.01.032>.
60. Cheung J, Rudolph MJ, Burshteyn F, et al. Structures of human acetylcholinesterase in Complex with pharmacologically important ligands. *J Med Chem*. 2012;55:10282–6. <https://doi.org/10.1021/jm300871x>.
61. Wang JL, Limburg D, Graneto MJ, et al. The novel benzopyran class of selective cyclooxygenase-2 inhibitors. Part 2: the second clinical candidate having a shorter and favorable human half-life. *Bioorg Med Chem Lett*. 2010;20:7159–63. <https://doi.org/10.1016/j.bmcl.2010.07.054>.
62. Sharma V, Bhatia P, Alam O, et al. Recent advancement in the discovery and development of COX-2 inhibitors: insight into biological activities and SAR studies (2008–2019). *Bioorg Chem*. 2019;89:103007. <https://doi.org/10.1016/j.bioorg.2019.103007>.
63. Lipinski CA, Lombardo F, Dominy BW, et al. Experimental and computational approaches to estimate solubility and permeability in drug discovery and development settings. *Adv Drug Deliv Rev*. 2001;46:3–26. [https://doi.org/10.1016/s0169-409x\(00\)00129-0](https://doi.org/10.1016/s0169-409x(00)00129-0).
64. Pires DE, Blundell TL, Ascher DB. pkCSM: predicting small-molecule pharmacokinetic and toxicity properties using graph-based signatures. *J Med Chem*. 2015;58:4066–72. <https://doi.org/10.1021/acs.jmedchem.5b00104>.
65. Mirzaei S, Eivand F, Hadizadeh F, et al. Design, synthesis and biological evaluation of novel 5, 6, 7-trimethoxy-N-aryl-2-styrylquinolin-4-amines as potential anticancer agents and tubulin polymerization inhibitors. *Bioorg Chem*. 2020;98:103711. <https://doi.org/10.1016/j.bioorg.2020.103711>.
66. Hasanin M, Hashem AH, El-Rashedy AA, et al. Synthesis of novel heterocyclic compounds based on dialdehyde cellulose: characterization, antimicrobial, antitumor activity, molecular dynamics simulation and target identification. *Cellulose*. 2021;28:8355–74. <https://doi.org/10.1007/s10570-021-04063-7>.
67. Machaba KE, Mhlongo NN, Soliman ME. Induced mutation proves a potential target for TB therapy: a molecular dynamics study on LprG. *Cell Biochem Biophys*. 2018;76:345–56. <https://doi.org/10.1007/s12013-018-0852-7>.
68. Cournia Z, Allen B, Sherman W. Relative binding free energy calculations in drug discovery: recent advances and practical considerations. *J Chem Inf Model*. 2017;57:2911–37. <https://doi.org/10.1021/acs.jcim.7b00564>.

Publisher's Note

Springer Nature remains neutral with regard to jurisdictional claims in published maps and institutional affiliations.